AIP | Applied Physics Letters

Engineering of gadofluoroprobes: Broad-spectrum applications from cancer diagnosis to therapy

Ranu A. Dutta, Prashant K. Sharma, Vandana Tiwari, Vivek Tiwari, Anant B. Patel, Ravindra Pandey, and Avinash C. Pandey

Citation: Applied Physics Letters **104**, 023703 (2014); doi: 10.1063/1.4861881
View online: http://dx.doi.org/10.1063/1.4861881
View Table of Contents: http://scitation.aip.org/content/aip/journal/apl/104/2?ver=pdfcov
Published by the AIP Publishing

Engineering of gadofluoroprobes: Broad-spectrum applications from cancer diagnosis to therapy

Ranu A. Dutta,[1,2,a)] Prashant K. Sharma,[1,3] Vandana Tiwari,[4] Vivek Tiwari,[5] Anant B. Patel,[5] Ravindra Pandey,[6] and Avinash C. Pandey[1,2,7]
[1]*Nanotechnology Application Centre, University of Allahabad, Allahabad 211002, India*
[2]*NanoeRA medicare Private Limited, Uttar Pradesh, India*
[3]*Indian School of Mines, Dhanbad, India*
[4]*Department of Pathology, KGMU, Lucknow, India*
[5]*Centre for Cellular and Molecular Biology, Hyderabad, India*
[6]*Department of Physics, Michigan Technological University, Michigan 49931-1295, USA*
[7]*Bundelkhand University, Jhansi, India*

(Received 1 May 2013; accepted 16 December 2013; published online 15 January 2014)

The engineering of the Gadolinium based nanostructures have been demonstrated in this paper. Nanostructures of α-Gd_2S_3 exhibit a unique transition between ferromagnetic state and paramagnetic state of the system. It was demonstrated that their properties could be tuned for a wide range of applications ranging from hyperthermia to Magnetic Resonance Imaging, owing to their magnetic moments and large relaxivities. Metallic Gd nanoparticles obtained by reduction method were employed for cancer imaging in mice. The Gd nanoparticles were coated with Curcumin and their biomedical implications in the field of simultaneous diagnosis and therapy of cancer and related diseases has been discussed. © *2014 AIP Publishing LLC*. [http://dx.doi.org/10.1063/1.4861881]

Rare earth based magnetic nanostructures have grabbed attention because of their distinct properties which make them desirable candidates for a large number of applications in field of medicine. Small change in the band structure of a solid, originating from nanoscale size, is expected to have significant effects on their magnetic properties. A wider variety of magnetic nanoparticles (MNPs) have been synthesized for biomedical applications.[1,2] The magnetic interactions at nanoscale are generally strong and can be modified to give suitable materials for such applications. In the past, Superparamagnetic Iron Oxide (SPIO)[3] and Ultra small superparamagnetic iron oxide (USPIO) have been mostly explored as magnetic vectors for drug delivery, Magnetic Resonance Imaging (MRI), Cell separation, etc. One of the most important applications among them is their use as contrast agents in MRI. These contrast agents consist of suspended colloids of iron oxide nanoparticles and when injected during imaging reduce the T2 (transverse relaxation) signals of absorbing tissues. As they are negative contrast they generate darker images which making it difficult to distinguish between diseased and normal tissues. To overcome this, positive contrast agents based on the rare earth metal Gadolinium have been explored since a few years. Among them Gd based chelates were the most popular candidates for such applications. These are chelates of Gd, namely, Gd DTPA (gadolinium-diethylenetriamine pentaacetic acid), Gd DOTA(1,4,7,10-tetraazacyclododecane-1,4,7,10-tetraacetic acid, DOTAREM (gadoterate meglumine), etc. Although they were capable of generation of positive contrast but their toxicities have been a matter of concern as Gadolinium is present in the free state, Gd^{3+}. Owing to the toxic nature of free Gd, Gd based nanoparticles have been explored since a few years. They showed better contrast compared to the Gd chelates owing to their nanosizes. The magnetic properties of rare earths[4–6] are found to be very sensitive to the structure and filling of the conduction bands because they originate almost entirely from their incomplete 4*f* shells. Since the emergence of Nanotechnology and the "Quantum Confinement Effect," these material systems need to be revisited as their magnetic properties could be enhanced by several folds in quantum confined regime. It is reasonable that when the paramagnetic molecules self-organize into an ordered microstructure, it would largely enhance the local magnetic moment of the formed particle when a foreign magnetic field is applied; such nanoparticles will enhance the relaxation of the water proton in MR imaging. This is achieved by the paramagnetic properties of the Gadolinium (III) ion stemming from its seven unpaired *f* electrons. This is consistent with the fact that if we want to increase the relaxation rate, we need to increase the number of Gd-ions by forming clusters of Gd-ions. Besides, if we can create nanoclusters where the electronic spins of the Gd-ions are also magnetically aligned, the relaxivity could be increased at least 1000 times.

Gadolinium ion loaded NPs,[7,8] gadolinium oxide NPs,[9] gadolinium hydroxide,[10] gadolinium fluoride NPs, and gadolinium loaded carbon nanohorn[11] have been investigated as alternative T1 MRI contrast agents and were found to have significant positive contrast effects. Another lanthanide ion, dysprosium (III), has recently been investigated as T2 contrast agent. Dy (III) has the highest effective moment among the lanthanides and thus the highest relaxivity. Norek *et al.* reported tuning the size of dysprosium oxide NPs for optimal performance as a T2 MRI contrast agent.[12] However, the applicability of most Gadolinium based contrast agents is still limited owing to the toxic nature of free Gadolinium.[13]

In this paper, the development of nanoparticles based on Gadolinium termed as gadofluroprobes has been reported. The nanostructures of Gadolinium sulphide (α-Gd_2S_3) have

[a)]E-mail: ranu.dutta16@gmail.com. Tel./Fax: +91-532-2460675.

been synthesized. To make these nanoparticles luminescent, Eu^{3+} ion was introduced into host α-Gd_2S_3 to obtain Luminescent magnetic quantum dots (LMQDs). Nanoparticles obtained by the alteration of synthesis methods resulted in significant changes in the properties of the material. A unique ferromagnetic to paramagnetic transition was recorded in these nanostructures. These properties of the material could be tuned for a wide range of applications ranging from hyperthermia to Magnetic Resonance Imaging.

The details about the synthesis methods for these nanoparticles and material characterization techniques employed have been described in Ref. 25. X-ray diffraction studies and Transmission electron microscopy support the formation of the nanoparticles of α-Gd_2S_3, represented in Figs. S1 and S2, respectively. The results of the magnetic characterization obtained by vibrating sample magnetometer, is shown in Fig. S3, see supplementary material. The graph shows a ferromagnetic behavior of the nanoparticles obtained by the first synthesis method, while by the second method a paramagnetic behavior was reported in Ref. 14. Hence, a transition between the ferromagnetic state and the paramagnetic state of this system was noticed. Furthermore, the origin and root cause of such strong magnetic behaviour of the host Gd_2S_3 nanoparticles were studied, see supplementary material for the electronic structure calculations of Gd_2S_3 cluster and fragments/nanostructures of α-Gd_2S_3 of various sizes.[25]

The relaxivities of these nanoparticles were calculated, the detailed process and parameters have been described in the supplementary material.[25] Relaxivity parameters (r_1, r_2) of Gd_2S_3:Eu^{3+} nanoparticles and Gd–DTPA were calculated from the slope of $1/T_1$ and $1/T_2$ graphs, shown in Figure 1. The relaxivity values, r_2 were obtained from the slopes of the linear fits of experimental data. The r_2 and r_1 values for Gd DTPA were 4.5 $mM^{-1}s^{-1}$ and 4.2 $mM^{-1}s^{-1}$, respectively, at higher Gd DTPA concentrations. While the r_2 and r_1 values for Gd_2S_3:Eu^{3+} were ~76 $mM^{-1}s^{-1}$ and ~45 $mM^{-1}s^{-1}$, respectively, indicating their efficacy at lower concentrations. The r_2/r_1 value of Gd_2S_3:Eu^{3+} nanoparticles is ~1.6, which is quite appropriate for a positive contrast agent. Gadolinium based probes are generally imaged with T_1 weighted sequences at standard clinical field strengths producing positive contrast. However, the R1 of these agents decrease rapidly at high field strengths reducing the sensitivity of these probes at high field. But in case of the gadofluoroprobes a very high R1 value was seen even at high magnetic field, indicating that the R1 value may be even greater at clinical field strength. The results of the bioimaging studies are shown in Figure 1(c). It gives a qualitative idea about the difference, in contrast, at different concentrations of the standard Gd DTPA and the synthesized LMQDs. It is evident that even at lower concentration a good contrast can be seen in the LMQDs sample.

To demonstrate the efficiency of the ferromagnetic nanoparticles for hyperthermia applications, experiments were conducted and the Specific Absorption Rate (SAR) was calculated, see supplementary material for experimental details and calculations.[25] It was observed that the time required to raise the temperature to 50 °C from room temperature was ~500 s for the suspension having a concentration of 20 μgml^{-1} of the synthesized luminescent nanomagnets, Fig. S5(a). Thus, even in presence of very low field (200 G) and with very small quantity (20 μgml^{-1}) of the synthesized LMQDs, the temperature could be raised up to 50 °C or above, in a very short period of time (<5 min).

As an illustration of the efficiency of the drug conjugated nanoparticles for cancer therapy, *in vivo* studies were performed on breast cancer cell lines (MCF 7), see supplementary material for cell studies.[25] Figure 2(a) shows the TEM image of untreated MCF 7 breast cancer cells. Most of the organelles are visible quite well; the nuclear membrane is distinct along with the mitochondria and lysosomes. The nucleus, nuclear membrane, nuclear pores, and some other organelles are visible very clearly. While in the TEM image, Figure 2(b), some nanoparticles seem to have entered the nuclear membrane and can be seen in the nucleoplasm. The organelles seem to have been destroyed and the condensed

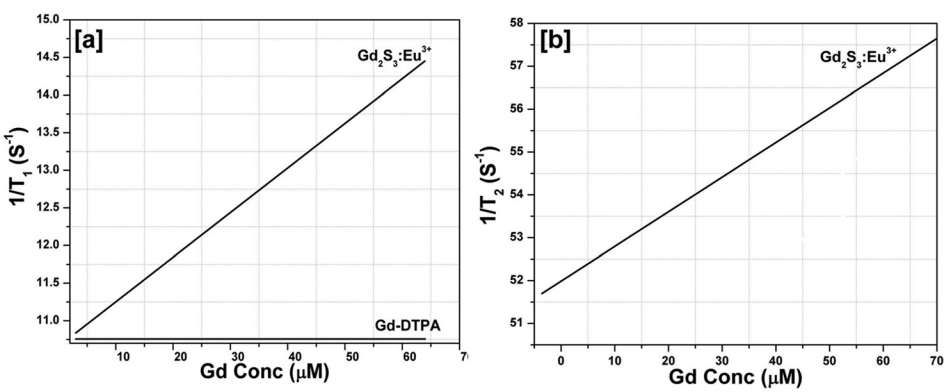

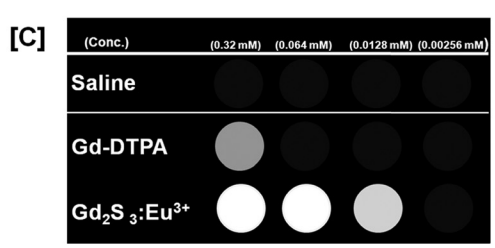

FIG. 1. (a) r_1 ($1/T_1$) relaxation rates of Gd DTPA and Gd_2S_3:Eu^{3+} nanoparticles, (b) r_2 ($1/T_2$) relaxation rates of Gd DTPA and Gd_2S_3:Eu^{3+} nanoparticles. (c) Bioimaging diagram of Gd_2S_3:Eu^{3+} nanoparticles.

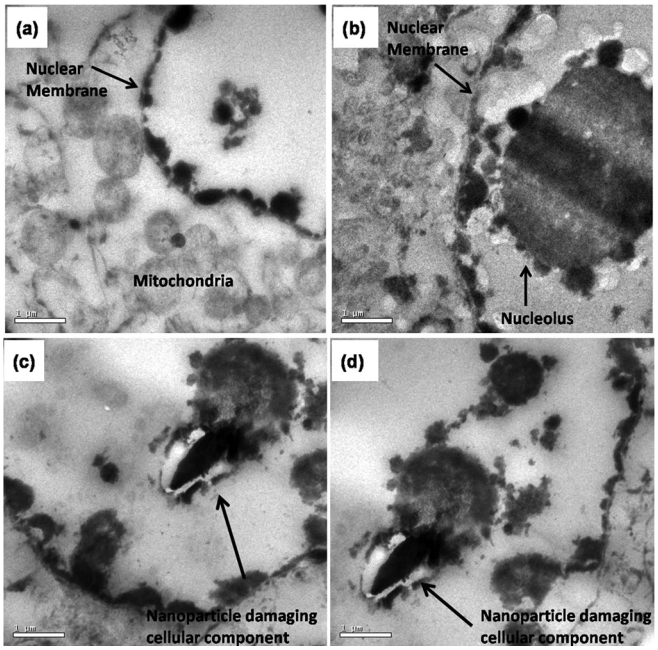

FIG. 2. TEM micrograph of (a) Untreated control MCF 7 cells, (b) drug conjugated LMQD treated, (c) and (d) Nanoparticle damaging cellular component.

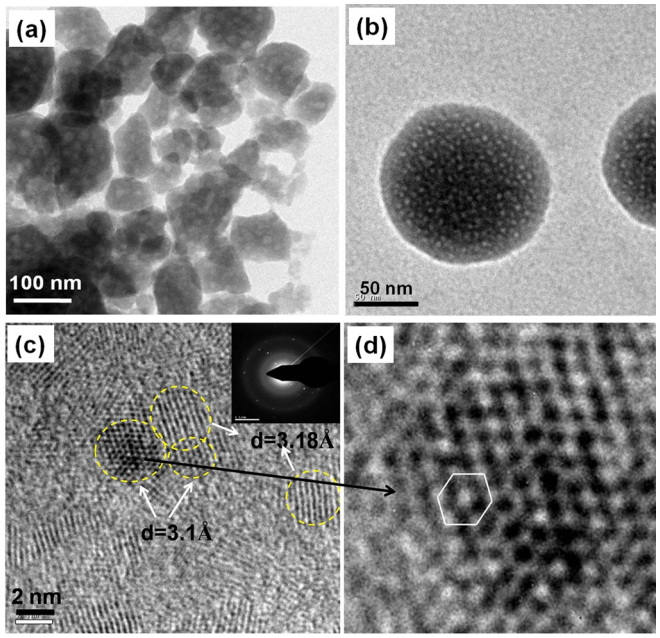

FIG. 3. TEM micrograph of (a) Metallo Gd-nanocongregates of size 100–150 nm composed of ultra small nanocrystals of size 3–5 nm, (b) Enlarged Metallic Gd-nanocongregate, (c) HRTEM images confirming the presence of ultra-small Gd-nanocrystals of size 3–5 nm. (d) Magnified view of (c) showing hexagonal atomic arrangement of the Gd-nanocrystals and inset of figure (c) shows SAED pattern of the same Gd-nanocrystal.

chromatin is indicative of apoptosis after the treatment (Figure 2(b)). This change in the structure could be attributed to the treatment of the cells with LMQDs. While Figures 2(c) and 2(d) both show the LMQDs treated breast cancer cells. In Figures 2(c) and 2(d), the rod shaped nanoparticles can be seen penetrating the cell and causing destruction like a nanobullet.

On the other hand, Gadolinium nanoparticles obtained by reduction of gadolinium salts possess very different properties compared to the Gd_2S_3 nanoparticles. Metallic Gadolinium nanoparticles were synthesized by a simple reduction method; see supplementary material for detailed synthesis method.[25] The TEM image in Figure 3(a) shows nano-congregates of nearly 100–150 nm size. Figure 3(b) shows a further magnified image of each nanocongregate, showing that each one is probably composed of ultra small nanocrystals, which have aggregated because of magnetic forces acting between them to form nano-congregates. This fact is further confirmed by Figure 3(c), which shows the high resolution transmission electron microscopic (HRTEM) image of these Gd- nanocongregates. HRTEM confirms the presence of ultra-small Gd-nanocrystals of size 3–5 nm. The observed lattice spacing is 3.1 Å, which corresponds to the hexagonal metallic Gd-nanoparticles grown in (100) direction. This observation is in accordance with the standard crystallographic data for metallic Gd [JCPDS No. 02-0864, having space group $P6_3/mmc$ (194) with primitive hexagonal crystal, cell parameters $a = b = 3.6$ and $c = 5.76$].[15–19] Figure 3(d) shows the further magnified image of Gd-nanocrystals depicting a very clear hexagonal atomic arrangement. Besides metallic Gd-nanocrystals, we also observe some of the nanocrystals having lattice spacing 3.18 Å–3.2 Å, which corresponds to (111) plane of monoclinic Gd_2O_3 [JCPDS No. 42-1465, having space group C2/m (12) with monoclinic structure].[20] This indicates that the synthesized samples contain few monoclinic Gd_2O_3 nanocrystals besides the hexagonal Gd-nanocrystals, which would have been be possible because of the diffusion of oxygen through the outer layer of some of the nanocrystals and would have oxidized them. In order to confirm the crystal structure of the prepared nanocrystals, selected area electron diffraction (SAED) was performed on the selected area of single Gd-nanocrystal. The SAED pattern shown in the inset of Figure 3(c), shows bright spot pattern, arranged in a hexagonal manner, which is because of the reflection/diffraction of electron beam from the (100) plane of the Gd-nanocrystals. This supports the synthesis of good crystalline Gd-nanocrystals.

The results of the relaxivity studies on Gd nanoparticles obtained through experiments are shown in Figure 4(a), for details see supplementary material.[25] The longitudinal relaxivity (*r1*) of the Gd-nanocrystals was calculated from the slope of R1 (1/T1) versus concentration graph. The *r1* value of the Gd-nanocrystals was found to be $3.57\,mM^{-1}s^{-1}$ (Figure 4(a)). In the T1 weighed image the Gd-nanocrystals solution look brighter than the saline. This is due to the reduction of the T1 relaxation times of water molecules by the Gd atoms in their vicinity. The standard Gd-DTPA solution appears darker than Gd-nanocrystals which is also in accordance with the relaxivity results. Inset shows the bioimages obtained in the clinical magnetic field of the 3 T MRI machine of saline and Gd DTPA. A good contrast could be seen in the nanoparticles suspension at a concentration of 0.25 mM, while no contrast could be seen in case of Gd DTPA at such low concentration. The homogeneous suspension of Gd nanocrystals was used for *in vivo* imaging studies on mice models, for details see supplementary material.[25] The mice induced with skin cancers were taken and imaged before and after injection of Gd nanocrystals suspension.

Figure 4 shows the sagittal MR images of mice before and after administration of the contrast agents. Figure 4(b)

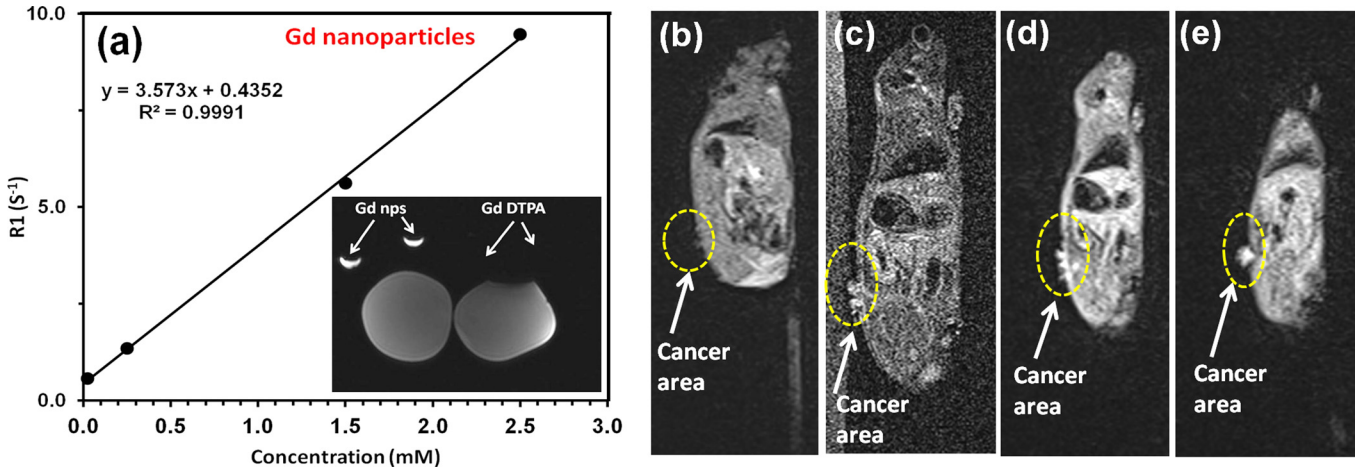

FIG. 4. (a) Relaxivity graph of the Gd-nanocrystals and inset shows bioimages of Gd-nanocrystals and Gd-DTPA in 3 Tesla clinical MRI Scanner at lower concentrations. Sagittal MRI images of mice (b) Pre-contrast (c) 2 min post contrast of Gd-DTPA (d) and (e) 2 min post contrast of Gd-nanocrystals.

shows image of mice without any contrast, Figure 4(c) shows mice imaged 2 min after administration of the conventional contrast agent Gd-DTPA, Figures 4(d) and 4(e) show mice imaged 2 min after administration of the synthesized Gd-nanocrystals based contrast agent. The tumor on the back of the mice is seen more clearly with the nanoparticles when compared to the standard contrast agent. See supplementary material for some of the axial view MRI images of mice with advanced stage cancer shown in Fig. S8.

In further experiments, the Gadolinium nanoparticles were coated with the curcumin molecules, changes in properties were studied and their possibilities for biomedical applications were discussed. Curcumin is a molecule, which plays a role in the cure of a wide range of diseases such as cancer, arthritis, inflammatory diseases, and other neurodegenerative diseases. Curcumin (diferuloylmethane) is the major active component of the food flavouring substance turmeric (Curcuma longa). Since years, turmeric has been used for many ailments, particularly, as an anti-inflammatory agent. However, the limitation to its practical application is due to the lack of its bioavailability in the body. The reasons for reduced bioavailability within the body are poor absorption, low intrinsic activity, high rate of metabolism, inactivity of metabolic products, and/or rapid elimination from the body. Studies to date have suggested a strong intrinsic activity and, hence, efficacy of curcumin as a therapeutic agent for various ailments.[21–23] Therefore, several attempts have been made for making nano formulations to overcome these problems. For example, Hailong Yu *et al*. have tried to increase the oral bioavailability of curcumin using organogel-based nanoemulsions.[24] It is estimated that the Gadolinium nanoparticles could act as magnetic carriers for these curcumin molecules and make them available at the target sites upon application of an external magnetic field, which could be employed for therapy as well as target specific imaging. The curcumin conjugated magnetic nanoparticles were obtained by the process shown schematically in Fig. S9, see supplementary material. The UV absorption spectra of the Gd nanoparticles and curcumin conjugated Gd nanoparticles have been shown in Fig. S10. Other than these, in the TEM image [Inset (b) of Figure 5] also it can be seen that some capping/coating has been done on the Gadolinium nanoparticles. HRTEM image shows the presence of small Gd-nanocrystals with lattice spacing 3.1 Å, which corresponds to the hexagonal metallic Gd-nanoparticles grown in (100) direction. In contrast to the earlier observation of bright spot pattern, arranged in a hexagonal manner in SAED, here in the inset (a) of Figure 5, we find broad diffused ring pattern in SAED, which is due to the coating of curcumin molecules on the surface of the Gd-nanocrystals. The *r1* relaxivity value has not changed much. A slight reduction was observed which could be due to the low water solubility of curcumin molecules resulting in reduced availability of water molecules in the vicinity of Gadolinium, hence reduction in relaxivity. The scope of the study lies in the future implication of this conjugate for a wide variety of biomedical applications such as imaging tumors, hyperthermia applications, and for release of the drug curcumin at the target site upon modulation of the magnetic field.

Thus, the paper exhibits the development of Gadolinium based probes and the tailoring of their properties by synthesis and functionalization with drug molecules for a wide range of biomedical applications. In case of Gd_2S_3 nanoparticles a unique transition between the ferromagnetic and paramagnetic properties was observed, depending upon which their possible

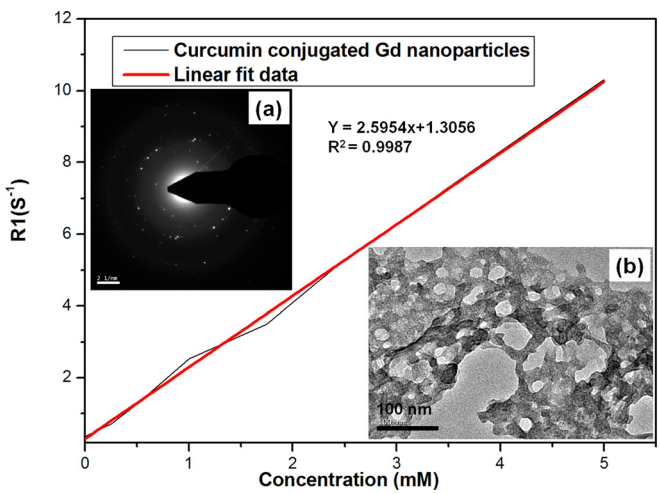

FIG. 5. Relaxivity graph of the Gd-nanocrystals conjugated to curcumin and inset (a) shows SAED pattern while inset (b) shows Transmission Electron Microscopic image.

biomedical applications have been demonstrated. Owing to their paramagnetic nature their application as a positive contrast agent in MRI has been shown, while their ferromagnetic behaviour has been exploited for hyperthermia and drug delivery applications on human breast cancer cell lines. It is known that Gadolinium demonstrates a magnetocaloric effect whereby its temperature increases when it enters a magnetic field and decreases when it leaves the magnetic field. Magnetic-field-induced excitations produce heat that increases the temperature of nanomagnets. Such specific heating represents an eliciting mechanism for the controlled release of conjugated drug molecules from the nanomagnets when they are heated to adequately high temperatures (around 40 °C). Hence, the simultaneous release of heat and also release of the drug molecule at the target site could be possible. It is well known that cancer growth stops at temperatures higher than about 42 °C. Besides, the efficiency of the drug conjugated nanoparticles against breast cancer cell lines has been demonstrated by various experiments. Methyl thiazol tetrazolium bromide (MTT) assay shows their cytotoxicity to cancer cells, while TEM studies show the uptake and internalization of the magnetic nanoparticles inside the cells and the resulting damage caused. The Gadolinium metallic nanoparticles possess distinct properties from those of Gd_2S_3 nanoparticles. The curcumin conjugated Gd nanoparticles could be applicable for imaging and therapeutic applications. Thus, the properties of the nanoparticles have been tuned in such a way that they can have a wide range of implications in diagnosis and therapy of cancer and may be useful for other related diseases subsequently. This work is under progress and the possibility of their implications in brain imaging is also being explored. These nanoparticles could be employed for small scale clinical trials after proper investigations.

The authors are thankful to Department of Science and Technology (DST), India and Defence Research and Development Organization (DRDO), India for supporting "Nanotechnology Application Centre" under "Nano-Mission (Grant No. SR/NM/NS-87/2008)" and (Grant No. ERIP/ER/1003852/M/01/1408) scheme of projects, respectively. We would like to extend our heartiest thanks to Dr. R. N. Bhargava, Nanocrystals Technology, NY, USA for his valuable discussions and suggestions throughout the work. For some facilitation during the experiments authors are thankful to Dr. Pradeep Kumar from NII, New Delhi and Dr. Jalaj Ajay Devgan, MMH College Gaziabad, New Delhi, Kriti Scanning Centre, Allahabad, India. The corresponding author is thankful to the MRI imaging facility of CCMB, Hyderabad. We would like to thank the animal ethical committee for granting permissions to carry experiments on mice.

[1]Q. A. Pankhurst, N. T. K. Thanh, S. K. Jones, and J. Dobson, J. Phys. D: Appl. Phys. **42**, 224001 (2009).
[2]D. L. Huber, Small **1**, 482 (2005).
[3]H. Gang, Z. Chunfu, L. Shunzi, K. Chalermchai, Y. Su-Geun, T. Ruhai, D. M. John, C. B. Kathlynn, and G. Jinming, J. Mater. Chem. **19**, 6367 (2009).
[4]J. C. Boyer, L. A. Cuccia, and J. A. Capobianco, Nano Lett. **7**, 847 (2007).
[5]J. S. Kim, W. J. Rieter, K. M. L. Taylor, H. An, W. Lin, and W. Lin, J. Am. Chem. Soc. **129**, 8962 (2007).
[6]J. Shen, L. D. Sun, and C. H. Yan, Dalton Trans. **2008**, 5687.
[7]R. K. Dutta, P. K. Sharma, and A. C. Pandey, Appl. Phys. Lett. **97**, 253702 (2010).
[8]S. Santra, R. P. Bagwe, D. Dutta, J. T. Stanley, G. A. Walter, W. Tan, B. M. Moudgil, and R. A. Mericle, Adv Mater. **17**, 2165 (2005).
[9]J. L. Bridot, A. C. Faure, S. Laurent, C. Rivière, C. Billotey, B. Hiba, M. Janier, V. Josserand, J. L. Coll, L. V. Elst, R. Muller, S. Roux, P. Perriat, and O. Tillement, J. Am. Chem. Soc. **129**, 5076 (2007).
[10]B. I. Lee, K. S. Lee, J. H. Lee, I. S. Lee, and S. H. Byeon, Dalton Trans. **2009**, 2490.
[11]J. Miyawaki, S. Matsumura, R. Yuge, T. Murakami, S. Sat, A. Tomida, T. Tsuruo, T. Ichihashi, T. Fujinami, H. Irie, K. Tsuchida, S. Iijima, K. Shiba, and M. Yudasaka, ACS Nano. **3**, 1399 (2009).
[12]M. Norek, G. A. Pereira, C. F. G. C. Geraldes, A. Denkova, W. Zhou, and J. A. Peters, J. Phys. Chem. C **111**, 10240 (2007).
[13]A. Li, C. S. Wong, M. K. Wong, C. M. Lee, and M. C. Yeung, Br. J. Radiol. **79**, 368 (2006).
[14]R. K. Dutta, P. K. Sharma, and A. C. Pandey, Sens. Transducers J. **122**, 36 (2010).
[15]R. M. Moon and W. C. Koehler, Phys. Rev. B **11**, 1609 (1975).
[16]B. Delley, J. Chem. Phys. **92**, 508 (1990).
[17]B. Delley, J. Chem. Phys. **113**, 7756 (2000).
[18]J. P. Perdew, Physica B **172**, 1 (1991).
[19]The International Centre for Diffraction Data® (ICDD®): JCPDS No. 02-0864, 1997.
[20]The International Centre for Diffraction Data® (ICDD®): JCPDS No. 42-1465, 1997.
[21]R. P. Sahu, S. Batra, and S. K. Srivastava, Br. J. Cancer **100**, 1425 (2009).
[22]Q. Zhou, X. Wang, X. Liu, H. Zhang, Y. Lu, and S. Su, Acta Pharmacol. Sin. **32**, 1402 (2011).
[23]J. H. Hong, K. S. Ahn, E. Bae, S. S. Jeon, and H. Y. Choi, Cell Death Dis. **4**, 505 (2013).
[24]H. Yu and Q. Huang, J. Agric. Food Chem. **60**, 5373 (2012).
[25]See supplementary material at http://dx.doi.org/10.1063/1.4861881 for some of the details for, e.g., materials/method/experimental protocols, characterization tools and techniques, simulation studies, hyperthermia studies, cell culture, and some mice imaging experiments, etc.